Nanoscale Advances

REVIEW

View Article Online
View Journal | View Issue

Cite this: *Nanoscale Adv.*, 2024, **6**, 5285

Recent developments in the bio-mediated synthesis of $CoFe_2O_4$ nanoparticles using plant extracts for environmental and biomedical applications†

Giang Thanh Tran,[ab] Luan Minh Nguyen,[cd] Thuy Thi Thanh Nguyen,[b] Dai Hai Nguyen [c] and Thuan Van Tran *[a]

Conventional methods for the synthesis of nanoparticles often involve toxic chemicals, exacerbating environmental issues in the context of climate change and water scarcity. Green synthesis using plant extracts offers a sustainable and viable alternative for $CoFe_2O_4$ nanoparticle production, but understanding the mechanisms and applications of this method is challenging. Here, we review the synthesis and applications of $CoFe_2O_4$ nanoparticles using plant extracts with emphasis on biomedical activity and water treatment. Plant extract-mediated $CoFe_2O_4$ nanoparticles exhibit high surface area, small particle size, unique morphology, sufficient band gap energy, and high saturation magnetization. These nanoparticles demonstrate strong antimicrobial and anticancer activities, highlighting their potential in biomedical treatments. Green $CoFe_2O_4$ are effective in removing organic dyes, heavy metals, and pharmaceuticals from water, promoting cleaner water resources. Challenges such as scalability and reproducibility still remain, but ongoing research aims to optimize synthesis protocols and explore new applications. This work underscores the importance of sustainable nanotechnology in addressing environmental challenges.

Received 22nd July 2024
Accepted 8th September 2024

DOI: 10.1039/d4na00604f

rsc.li/nanoscale-advances

1. Introduction

Recently, the trend of synthesizing green magnetic ferrite nanoparticles *via* biological routes has shown promising potential to gradually replace traditional synthesis methods (physical and chemical methods).[1] Many studies on the green synthesis of various magnetic ferrites, such as $NiFe_2O_4$, $CuFe_2O_4$, $MnFe_2O_4$, $ZnFe_2O_4$, and $CoFe_2O_4$, highlight their application possibilities in diverse fields including sensors, catalysts, batteries, drug carriers, and supporting agents in biomedical engineering.[2–5] The common characteristics of these green synthesis methods are their environmental friendliness, reduced harm to human health, and lower costs compared to traditional methods. The synthesis of green magnetic ferrite nanoparticles can be facilitated by various sources, including bacteria, fungi, and plants.[6–8] Differences in Fe precursors, natural raw sources, and experimental conditions lead to variations in the physicochemical properties of magnetic ferrite nanoparticles, such as particle size, surface area, optical properties, and magnetic properties.[9] These variations result in different types of divalent and trivalent ion occupations in the tetrahedral and octahedral sites of magnetic ceramide structures, including normal spinel ferrite ($ZnFe_2O_4$),[10] and inverse and mixed spinel ferrites ($NiFe_2O_4$, $CuFe_2O_4$, $MnFe_2O_4$, $CoFe_2O_4$).[11] Furthermore, inverse spinel ferrite is considered one of the magnetic ceramides with more outstanding properties such as superparamagnetism, low toxicity, easy magnetic separation from the reaction medium, and biocompatibility.[12] Among the various spinel ferrites, $CoFe_2O_4$ stands out as a highly attractive magnetic material due to its specific properties and promising applications in biomedicine, agriculture, and industries.[13]

In the past decade, the research and development of cobalt ferrite nanoparticles through biological methods have garnered increasing attention from researchers. Notably, studies have been conducted to synthesize cobalt ferrite nanoparticles from a variety of natural materials, which are environmentally friendly and more cost-effective. For instance, extracellular synthesis processes of $CoFe_2O_4$ nanoparticles from fungi such

[a]*Institute of Applied Technology and Sustainable Development, Nguyen Tat Thanh University, 298-300A Nguyen Tat Thanh, District 4, Ho Chi Minh City 755414, Vietnam. E-mail: tranuv@gmail.com; tranvt@ntt.edu.vn; Fax: +84-28-39-404-759; Tel: +84-28-3941-1211*

[b]*Nong Lam University Ho Chi Minh City, Ho Chi Minh City 700000, Vietnam*

[c]*Institute of Chemical Technology, Vietnam Academy of Science and Technology, 1A TL29, District 12, Ho Chi Minh City, 700000, Vietnam*

[d]*Graduate University of Science and Technology, Vietnam Academy of Science and Technology, Hanoi, 100000, Vietnam*

† Electronic supplementary information (ESI) available. See DOI: https://doi.org/10.1039/d4na00604f

as *Aspergillus nidulans* and *Monascus purpureus* have been explored.[14,15] Among biological pathways, synthesizing $CoFe_2O_4$ nanoparticles with the help of plant extracts accounts for the majority of reports. This synthesis process can utilize various plant species and almost every part of the plant, including roots, stems, branches, leaves, bark, and fruit.[16–19] Furthermore, the $CoFe_2O_4$ nanoparticles synthesized from these biological pathways show potential applications in fields such as antioxidants,[15] anticancer drugs,[15] electrochemistry,[4] catalysts,[14] and magnetic resonance imaging.[20] The production and application potential of green $CoFe_2O_4$ nanoparticles indicate the possibility of replacing traditional methods of synthesizing $CoFe_2O_4$ nanoparticles. Particularly, with the support of plant extracts, this approach holds promise as a viable alternative due to its cost-effectiveness and environmental benefits.

Indeed, the green synthesis of $CoFe_2O_4$ nanoparticles from plant extracts brings many benefits, such as being environmentally friendly, less harmful to humans and animals, easy to perform, cost-saving, and not requiring complicated machinery. Firstly, phytochemicals in plant extracts can replace toxic solvents, *e.g.*, urea, benzyl ether, octanol, and NaOH, or surfactants peracetic acid, polyvinylpyrrolidone,[21] which are commonly used in chemical synthesis. These phytochemicals have been shown to function as complexing, capping, and stabilizing agents in the formation of $CoFe_2O_4$ nanoparticles.[22] Secondly, the phytochemicals in plant extracts are environmentally friendly and benign to humans, ensuring that the synthesis process does not harm human health. Thirdly, the synthesis of green $CoFe_2O_4$ nanoparticles is straightforward and does not require many processes or complicated steps compared to methods such as sonochemical, sol–gel, and combustion synthesis.[21] Finally, thanks to these advantages, scaling up the industrial production of green $CoFe_2O_4$ nanoparticles offers promising prospects for a method that meets green chemistry standards while demonstrating high application efficiency.

While numerous studies have explored the structural characteristics and applications of $CoFe_2O_4$ nanoparticles, research gaps are remaining, specifically addressing ferrite cobalt-based nanoparticles synthesized from plant extracts. For instance, Ameen and Majrashi[23] examined the antimicrobial properties of $CoFe_2O_4$ nanoparticles synthesized through biological and chemical pathways, yet did not delve into the factors influencing their structural characteristics or formation mechanism of $CoFe_2O_4$ nanoparticles. Moreover, the discussions of $CoFe_2O_4$ nanoparticles biosynthesized using plant extract were limited. In another study, Barani *et al.*[24] focused on evaluating the theranostic potential of $CoFe_2O_4$ nanoparticles in drug delivery, hyperthermia, contrast agents, and cell tracking, but did not extensively cover synthesis conditions and physicochemical properties. The role of bio-mediated $CoFe_2O_4$ nanoparticles in biomedical fields was not thoughtfully presented. Similarly, Sonu *et al.*[25] concentrated on individual photocatalytic applications of $CoFe_2O_4$ nanoparticles synthesized primarily through conventional methods such as co-precipitation, hydrothermal, and sol–gel. Although Katoch *et al.*[26] detailed synthesis procedures, physicochemical properties, and applications of $CoFe_2O_4$ nanoparticles in electronic devices, microwave devices, and wastewater treatment, these aspects were briefly assessed. In other studies, Xuan *et al.*[27] and Ahmad and Zhou[28] have explored the effect of specific properties like microwave absorption and toxicity on biomembranes, biomolecules, and immune systems of $CoFe_2O_4$-based nanocomposites, but these were limited to chemically synthesized materials.

This study aims to offer insights into the synthesis of $CoFe_2O_4$ nanoparticles using plant extracts, assess their structural characteristics, and discuss potential applications across various fields. Also, we explore the diversity of natural raw materials utilized in synthesis, underscore the advantages of using plant extracts, and elucidate specific mechanisms involved in the formation of green $CoFe_2O_4$ nanoparticles. Finally, the present review highlights prospects and limitations of plant extract-synthesized $CoFe_2O_4$ nanoparticles for sustainable development goals.

2. Structure and biosynthesis of $CoFe_2O_4$ nanoparticles

2.1. Structure and potential of $CoFe_2O_4$ nanoparticles

The structural lattice of cobalt ferrite, a well-known inverse spinel ferrite in the family of ceramic-magnetic nanoparticles, involves the occupation of all Co^{2+} ions on 16 octahedral sites, while Fe^{3+} is equally distributed between 8 tetrahedral and remaining octahedral sites.[11,29] The cation distribution among tetrahedral and octahedral sites of a spinel lattice can be determined by octahedral site preference energies of the cations.[11] The variation in crystal field stabilization energies results in the degree of inversion, and diverse characteristics of cobalt ferrite, including magnetic ordering, ferrimagnetic behavior, and superparamagnetic behavior.[11] $CoFe_2O_4$ demonstrates outstanding physical and chemical properties such as good mechanical hardness, high coercivity, shielding efficiency, wear anisotropy, ac-conductivity, high mechanical strength, dielectric constant and loss, moderate saturation magnetization, high chemical stability, high magneto-crystalline anisotropy, large magneto-crystalline anisotropy constant, and the high temperature of magnetic ordering (520 °C).[13,30,31]

Thanks to its excellent magnetic properties, $CoFe_2O_4$ is used in a variety of fields. In biomedicine, $CoFe_2O_4$ is beneficial for magnetic hyperthermia treatment of cancer,[32] drug delivery,[33] magnetic resonance imaging,[34] and antimicrobial activity.[35] The major advantages of $CoFe_2O_4$ are to induce local heat under an external alternating magnetic field at tumor sites,[36] act as a good contrast agent due to its magnetization properties and long circulation times,[34] and possess unique properties, *e.g.*, high hydrophilic, high permeability, low dielectric loss, and constant magnetization.[34,37,38] In the field of sensors, $CoFe_2O_4$ with high selectivity and sensitivity serves as a promising biosensor and physical–chemical sensor.[3] For wastewater treatment, this ferrite is capable of adsorbing and photodegrading contaminants thanks to its good chemical surface and capability to perform advanced oxidation processes.[39] $CoFe_2O_4$ also acts as

a heterogeneous catalyst in organic reactions such as dehydrogenation, oxidation, alkylation, and C–C coupling.[40] Moreover, $CoFe_2O_4$ has been applied in high-density data storage and energy storage devices like supercapacitors, batteries, lithium-ion batteries, and hydrogen production since this material offers high theoretical capacity, multiple redox reactions, enhanced chemical stability of electrodes, low cost, and environmental friendliness.[41,42] $CoFe_2O_4$ nanoparticles are also effective for absorbing or reflecting radiations in electromagnetic interference shielding, while being lightweight, corrosion-resistant, and easy to process. By possessing excellent magnetic and mechanical properties, $CoFe_2O_4$ shows great potential in various applications, giving rise to extensive research on methods to produce $CoFe_2O_4$ with specific properties suitable for each application. This aspect includes both conventional methods such as physical or chemical methods, and green synthesis methods based on green chemistry standards.

2.2. Conventional and green synthesis of $CoFe_2O_4$ nanoparticles

The variety of traditional methods in the synthesis of $CoFe_2O_4$ nanoparticles leads to differences in the formation of inverse or mixed-type cobalt ferrite.[43] Variations in crystal structure characteristics due to changes in synthesis factors such as temperature, time, synthesis solvent, and reactant also bring out inhomogeneities in physicochemical properties such as magnetic, optical, thermal, and electrical properties of $CoFe_2O_4$ nanoparticles.[30] These variations, such as the spin canting effect, spin-glass-like behavior, superparamagnetic properties, and higher heat and corrosion resistance, have also enabled diverse applications of $CoFe_2O_4$ in many fields.[43,44] Although traditional methods of $CoFe_2O_4$ synthesis offer applicability in various scientific and technical fields, stability issues, and limitations such as environmental impact and energy consumption hinder their industrial-scale synthesis.[45] For instance, methods like microwave, hydrothermal, sol–gel, co-precipitation, micro-emulsion, solid-state, refluxing, and ball-milling require multiple steps, use organic solvents, may result in impurities, require longer synthesis times, and consume significant energy.[30,46]

To mitigate the disadvantages of traditional synthesis methods, the green synthesis of $CoFe_2O_4$ nanoparticles through biological routes is considered one of the most eco-friendly, inexpensive, and assessable methods. This approach minimizes the use of harmful solvents and energy consumption, making it suitable for large-scale production while maintaining environmental sustainability. Green synthesis of $CoFe_2O_4$ nanoparticles using plant extracts through biological pathways has yielded many positive results in terms of internal properties and is widely applied in diverse fields. According to Velayutham *et al.*,[47] green $CoFe_2O_4$ nanoparticles were successfully synthesized using *Hibiscus rosa-sinensis* leaf extract, yielding nanoparticles with outstanding properties, such as a low bandgap energy of approximately 2 eV and a magnetization value exceeding 104 emu g^{-1}. The diverse morphology of $CoFe_2O_4$ nanoparticles can range from spherical to polyhedral shapes, such as cubic or rhombus bipyramid, all on a nano-sized scale (Table S1†). This morphological diversity depends on the specific plants used in the synthesis process, which can include *Syzygium aromaticum* leaf, *Moringa oleifera* leaf, *Tamarindus indica* fruit, and so forth.[48–50]

Several critical evaluations between conventional and green synthesis of $CoFe_2O_4$ nanoparticles can be pointed out as follows. Traditional synthesis methods, such as the wet chemical routes, *e.g.*, autocombustion, sol–gel, co-precipitation, and hydrothermal, require a substantial amount of chemicals, *e.g.*, NaOH or KOH to create a concentrated alkaline environment and surfactants to lessen surface tension. Additionally, these processes often necessitate high temperatures, sometimes reaching up to 1300 °C, and long synthesis times ranging from 5 to 12 h.[51,52] On the other hand, physical routes, *e.g.*, ball-milling and conventional ceramic methods, demand complex machinery capable of generating pressures up to 5 GPa.[53,54] These methods are not only energy-intensive but also time-consuming.

In contrast to harmful and expensive chemicals for conventional synthesis, raw materials of green synthesis method are locally available. The plant species are present in almost every geographical location on the earth, and show great potential for exploiting and applying them in the green synthesis of $CoFe_2O_4$. Extracts from plant parts can be easily obtained using water as a solvent and used directly to support the synthesis of $CoFe_2O_4$ (Fig. 1). Another advantage of this method is the diversity of phytochemical compounds in plant parts, including roots, bark, stems, branches, leaves, fruit, and husks, providing numerous options for the synthesis process, reducing production costs, and increasing the accessibility of the method.[55,56] Phytochemicals act as natural complexing, capping, and stabilizing agents in the green synthesis of nanoparticles. This helps to minimize or completely eliminate the addition of toxic fuels, additives, surfactants, and solvents, typically, urea, peracetic acid, benzyl ether, benzene sulphonates, and sodium dodecyl in the traditional synthesis of $CoFe_2O_4$.[57] By substituting plant extract-derived green solvents for organic solvents, the synthesis of $CoFe_2O_4$ is simplified, easier to perform, and meets the green synthesis requirements for application and production.[58]

Given these challenges, the green synthesis route for synthesis of $CoFe_2O_4$ should be prioritized for sustainable development goals. The green approach utilizing plant extracts and biological pathways offers a more environmentally friendly, cost-effective, and scalable alternative to traditional physical and chemical synthesis methods.

2.3. Abundancy of plant raw materials

The richness and diversity of plants, along with their resilience, is a key factor in promoting ecosystem dynamics in the research and development of scientific and productive sectors. Plant diversity can be observed in terms of species richness, species evenness, genetic diversity, and functional diversity. For example, the Amazon rainforest boasts an incredible diversity of plant species, containing more than 16 000 tree species and many understory plant species, demonstrating as a rich source

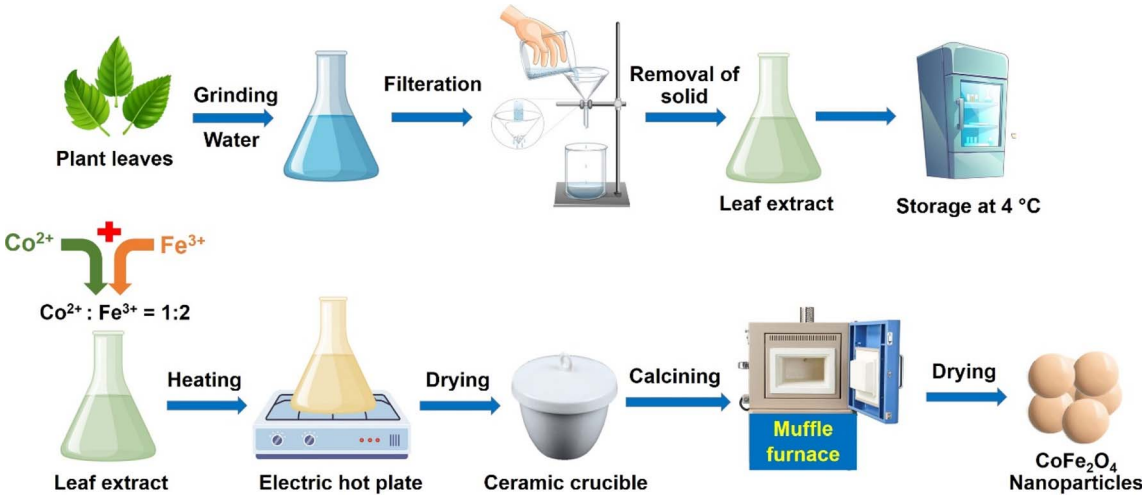

Fig. 1 The preparation of leaf extract and $CoFe_2O_4$ nanoparticles using leaf extract.

of inputs for the environmentally friendly, green production processes.[59] Furthermore, the richness of plant species indicates the widespread existence of these species in various regions of the earth, with a homogeneous distribution of some plant types, ranging from woody plants to herbaceous plants, and from perennial plants to short-term plants.

Moreover, the natural genetic diversity in plant species during growth and development contributes to an increasing number of species, thereby enhancing the diversity of input material sources. Globally, plant diversity follows distinct patterns, with tropical regions such as the Congo Basin boasting unparalleled species richness and functional diversity due to stable climates and complex ecological interactions.[60] Because of their ability to survive in a variety of environments and their large number of species, plants are considered excellent candidates for input materials. Specifically, during the production of materials such as $CoFe_2O_4$ nanoparticles, the use of plants or plant extracts to gradually replace toxic solvents is considered a top strategic priority. This approach not only supports sustainable production nano practices but also leverages the vast potential of plant diversity to innovate and improve green synthesis methods.

Table S1† illustrates how a range of plants are employed to promote the synthesis of cobalt ferrite nanoparticles and various parts of the plant can be utilized in the extraction process. Notably, leaf extracts are used in over 45% of relevant studies to aid in the manufacture of cobalt ferrite nanoparticles (Fig. 2). The remaining proportion of reports is distributed evenly among other plant parts, including the stem, flower, fruit, root, and seed. This preference for leaf extracts can be attributed to their easy accessibility compared to other plant parts. Leaves are often abundant, readily available, and can be sustainably harvested without causing significant harm to the plant. The abundance and variety of phytochemicals in leaf extracts, such as polyphenols, flavonoids, and alkaloids, serve as effective capping and complexing agents.[61] These compounds facilitate the complex formation process, making it more efficient and stable. Extraction processes prioritize leaves due to their abundance, ease of harvesting, year-round availability, and multiple harvesting opportunities. While other plant parts also contain diverse biological compounds crucial for forming complexes between precursor ions and phytochemicals, they present more limitations in terms of accessibility and harvesting. Harvesting stems and roots requires removing the entire plant, which is not sustainable for repeated cycles. Flowers, fruits, and seeds allow more sustainable extraction, but these parts must be harvested at the appropriate time and often do not yield as much as leaves. Therefore, leaf extraction is prioritized in the green synthesis of $CoFe_2O_4$ nanoparticles, ensuring the smoother and more efficient production process.

Notably, thanks to the diversity of phytochemical molecules in the extracts of certain plants, the green synthesis of $CoFe_2O_4$

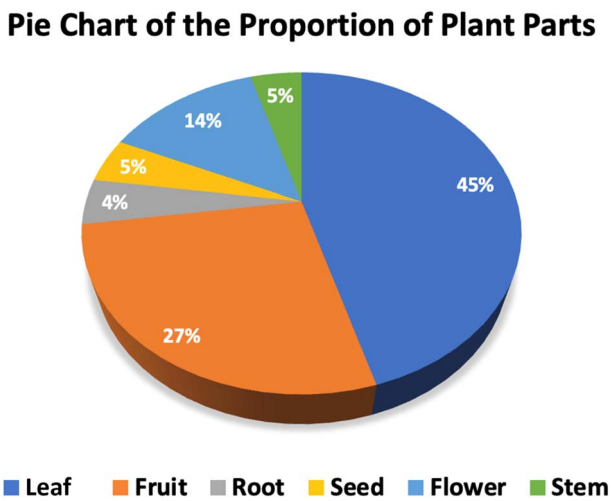

Fig. 2 A pie chart of the proportion of plant parts used for synthesizing green cobalt ferrite nanoparticles. Note: data were collected from the relevant references cited in this work.

nanoparticles is evaluated extensively (Table S1†). These studies have provided substantial evidence for replacing traditional methods and their potential for scalability to an industrial level. For instance, the flowers and leaves of *Hibiscus rosa-sinensis* contain a rich variety of biological compounds such as phenolic acids, flavonoids, and anthocyanins.[62,63] Such diversity has led to several published reports on the successful synthesis of $CoFe_2O_4$ nanoparticles from *Hibiscus rosa-sinensis* extract, demonstrating their potential applications in various fields, including biomedicine and wastewater treatment.[47,62] Another widely used plant in nanoparticle synthesis is *Aloe vera*. The leaf extract of this plant is rich in potent polyphenols, organic acids, and various polysaccharides.[64] These capping and chelating agents facilitate the green synthesis of $CoFe_2O_4$ nanoparticles through various methods, including sol–gel, autocombustion, hydrothermal, and microwave techniques.[64–66] The utilization of such diverse plant extracts underscores the versatility and effectiveness of green synthesis methods. As such, green methods not only provide an environmentally friendly alternative to traditional synthesis routes but also exhibit potential for large-scale production, thereby promoting sustainable development in various scientific and industrial applications.

One of the outstanding advantages of synthesizing $CoFe_2O_4$ nanoparticles from plant extracts is that plant biowastes can be converted into biological input for the extraction process. Utilizing waste sources for the synthesis of $CoFe_2O_4$ nanoparticles or $CoFe_2O_4$ hybrid nanocomposites not only helps treat waste that could potentially pollute the environment but also converts these waste sources into valued agents that support green synthesis. Indeed, agro-industrial waste from agricultural and industrial activities creates a significant burden by contributing to pollution from post-production processes. The agricultural sector alone is responsible for up to 21% of greenhouse gas emissions.[67] Each year, thousands of metric tons of peels, oil cakes, husks, leaves, stems, roots, seeds, and flowers pose risk when released into the environment without proper ecological treatment.[68] Therefore, many studies aim to process and convert these waste resources into useful products or materials. For instance, to address the large amount of waste from *Nephelium lappaceum* L. peels, Rahmayeni *et al.*[69] evaluated the ability of *Nephelium lappaceum* L. peel extract to support the synthesis of $CoFe_2O_4$ nanoparticles and $CoFe_2O_4$/ZnO nanocomposites. Both $CoFe_2O_4$ nanoparticles and $CoFe_2O_4$/ZnO nanocomposites synthesized by this way exhibited good electrochemical and magnetic properties, showing strong performance as photocatalysts.[69] In another report, Tatarchuk *et al.*[70] successfully synthesized inverse spinel $CoFe_2O_4$ nanoparticles from grape peel extract, demonstrating good catalytic activity in decomposing hydrogen peroxide *via* the Fenton process. These results highlight the great potential of the green synthesis of $CoFe_2O_4$ nanoparticles using plant extracts, offering a solution for agricultural waste while providing a safer, more economical, and environmentally sustainable method for material synthesis.

2.4. Role of plant extracts

Over the past two decades, the number of studies on using plant extracts for synthesizing metal/metallic nanoparticles such as Ag, Au, Al_2O_3, ZnO, ZrO_2, magnetic ferrite, and others has increased, and the intrinsic properties of several plant extract-mediated nanomaterials often show superior capabilities or properties compared to those synthesized by physical and chemical methods.[1,71] This advantage can rely on the presence of biological compounds in plants, which are estimated to be of more than 200 000 types.[72] Each phytochemical compound has a different operating mechanism as reducing, stabilizing, and capping agents for the synthesis process of various metal, or metal oxide nanoparticles. However, the specific role of each phytochemical underlying the formation of green nanoparticles still remains relatively inconsistent or unreported. It can be understood that the molecules such as polyphenols, alkaloids, flavonoids, terpenoids, and enzymes have different functional groups, showing varied reducing and capping roles.

Regarding the formation of $CoFe_2O_4$ nanoparticles, the complexing and capping functions of phytochemicals stabilize the complexes between precursor ions (Co^{2+}, Fe^{3+}) and biosubstances. These functions lead to more effective nucleation and crystal growth, thereby, reducing aggregation and maintaining uniformity in particle sizes of $CoFe_2O_4$ nanoparticles. For example, Kombaiah *et al.*[45] evaluated the distribution of $CoFe_2O_4$ nanoparticle size through conventional heating and microwave-assisted combustion methods using extracts from *Abelmoschus esculentus*. The results showed that the microwave-assisted method synthesized $CoFe_2O_4$ nanoparticles with smaller sizes ranging from 5 to 50 nm, whereas the conventional heating method resulted in particle sizes mainly between 300 and 500 nm. This difference is attributed to the capping agents found in phytochemicals. In the conventional combustion method, the high calcination temperatures allow most capping agents to be decomposed, leading to increased and uneven particle sizes. Conversely, in microwave-assisted combustion methods, most capping agents in the plant extract remain present due to the heating process at a lower temperature.

Differences in functional groups, *e.g.*, –OH, $–NH_2$, *etc.*, on aromatic compounds, aldehydes, esters, and ethers lead to varied interactions, *e.g.*, chelation and complexation between precursors and phytochemicals. However, the role of interactions during the $CoFe_2O_4$ nanoparticle synthesis process is still under investigation. To sum up, the plant extracts play a significant role in the green synthesis, and their utilization could significantly advance the development of sustainable materials. This approach aligns with the principles of green chemistry, aiming to reduce or eliminate the use of hazardous substances in the design, manufacture, and application of $CoFe_2O_4$ nanoparticles.

2.5. Formation mechanism of plant extract-mediated $CoFe_2O_4$ nanoparticles

Hypothetical theories that propose the most accurate and suitable mechanism for the synthesis of metal ferrite

nanoparticles, specifically $CoFe_2O_4$ nanoparticles from plant extracts, still face controversy regarding consistency across studies. However, the presence of phytochemicals in plant extracts has been shown to be crucial in the formation of $CoFe_2O_4$ nanoparticles. Functional groups such as carboxylic, hydroxyl, ether, ester, and others in phytochemical molecules can form complexes with precursor ions.[73] These biomolecules act as complexing and capping agents, facilitating the formation of (Co^{2+} Fe^{3+})-phytochemical complexes. Depending on the synthesis method (thermolysis, hydrothermal, co-precipitation, sol–gel, *etc.*) and specific conditions (temperature, pressure, precursor/solvent ratio, time), variations in the formation mechanism of $CoFe_2O_4$ nanoparticles occur.

First of all, temperature variations during the synthesis of $CoFe_2O_4$ nanoparticles significantly influence the phase determination in the primary synthesis mechanism. For example, the synthesis of $CoFe_2O_4$ nanoparticles *via* thermolysis occurs at high temperatures above 300 °C. This method involves two main steps: the nucleation process and the growth of $CoFe_2O_4$ on these homogeneous nuclei. Since the thermolysis process temperature is below 250 °C, the reaction does not fully decompose the mixed (Co^{2+} Fe^{3+})-complexes, leading to the formation of only a few $CoFe_2O_4$ nuclei (with monomer concentration below the critical concentration). Consequently, these few $CoFe_2O_4$ nuclei are unstable and can readily dissolve again.[74] However, the thermolysis process at temperatures higher than 300 °C occurs with complete decomposition of the mixed (Co^{2+} Fe^{3+})-complexes, resulting in the creation of a large number of $CoFe_2O_4$ nuclei. The growth of $CoFe_2O_4$ molecules on these $CoFe_2O_4$ nuclei is robust, leading to the formation of $CoFe_2O_4$ nanoparticles.[74] Overall, while the exact mechanisms remain under debate, it is evident that temperature is a critical factor influencing the synthesis outcome.

As $CoFe_2O_4$ nanoparticles are synthesized by the hydrothermal method, the reaction temperature is usually lower than 200 °C. At this temperature, the formation of $CoFe_2O_4$ nanoparticles is less influenced by temperature and more dependent on the chelating agents present in the reaction mixture. The knowledge about the formation mechanisms of cobalt ferrite nanoparticles in hydrothermal fluids is surprisingly limited. The plausible formation mechanisms of $CoFe_2O_4$ nanoparticles are attributed to chelating agents, which form (Co^{2+} Fe^{3+})-complexes.[75] The next step involves the decomposition of (Co^{2+} Fe^{3+})-complexes and the formation of $CoFe_2O_4$ nanoparticles under high pressure for an extended period.[76] The process of synthesizing $CoFe_2O_4$ nanoparticles from plant extract *via* the hydrothermal method has shown similar results. Thanks to the chelating agents in the plant extract, which facilitate the formation of $CoFe_2O_4$ nanoparticles, Hermosa *et al.*[65] and Baytar *et al.*[77] have successfully synthesized green $CoFe_2O_4$ nanoparticles in the temperature range of 180–220 °C over a period of 6–12 h. This finding can be explained as the carboxyl and hydroxyl functional groups present in the phytochemical molecular structure form coordinated bonds with Fe^{3+} and Co^{2+} ions through electron pair donations from these functional groups.

In addition, the synthesis of $CoFe_2O_4$ nanoparticles is also carried out using microwaves to support the formation of $CoFe_2O_4$ nanoparticles through the simplified process with significantly shortened times. One of the most advantageous features of the microwave-assisted method is reduction of the synthesis time from several hours to just 10–15 min.[64,78] The efficiency of microwave method relies on the power of microwave irradiation, which heats the material from within by transferring energy directly to the molecules. Upon receiving microwave energy, the molecules oscillate around their fixed positions, increasing the rate of molecular collisions. This causes the reaction heat to rise rapidly and disperse evenly throughout the system. The solution first reaches its boiling point through dehydration, followed by the evolution of large quantities of gases *via* complex decomposition. Finally, the reaction reaches the point of spontaneous combustion, where the components in the solution receive substantial heat, initiating robust evaporation and the formation of solid phases, ending up the synthesis process.[79]

Considering the efficiency of the microwave-assisted method compared to conventional heating methods, the microwave combustion method shows great potential for saving costs and time in synthesizing $CoFe_2O_4$ nanoparticles. For example, Kombaiah *et al.*[78] synthesized $CoFe_2O_4$ nanoparticles from *Opuntia dillenii* haw extract using both microwave combustion and conventional combustion methods. The results showed that the conventional combustion method required a heating temperature of up to 1000 °C and a total time of up to 6 h. In contrast, the microwave combustion method required only the boiling point temperature of the components and a synthesis time of about 15 min.[78] The potential of the microwave combustion method for synthesizing $CoFe_2O_4$ nanoparticles is evident as it saves energy, reduces synthesis time, and operates in a simple and safe manner, compared to the conventional combustion method.

3. Properties of plant extract-synthesized $CoFe_2O_4$ nanoparticles

3.1. Surface area

The synthesis conditions and methods used for producing $CoFe_2O_4$ nanoparticles result in significant variations in the specific surface area of the $CoFe_2O_4$ nanoparticle-based composites. Although these approaches utilize plant extracts, differences in the type of extract and synthesis steps lead to variations in the specific surface area of the $CoFe_2O_4$ nanoparticles, which do not follow a consistent trend. Evaluating the effect of calcination on the synthesis of $CoFe_2O_4$ nanoparticles at the same temperature and time reveals that an increase in surface area often corresponds to an increase in particle size, in contrast to the typical expectation that smaller particle sizes yield larger surface areas. For example, Manikandan *et al.*[64] synthesized $CoFe_2O_4$ nanoparticles from *Aloe vera* leaf extract at 500 °C for 2 h, resulting in a surface area of 73 m^2 g^{-1} and a particle size of 27 nm. Under similar conditions, Punyasamudram *et al.*[19] synthesized $CoFe_2O_4$ nanoparticles using

Carissa carandas stem extract, achieving a surface area of 136 m^2 g^{-1} and an average particle size of 35 nm. A similar trend is observed in the microwave-assisted synthesis of green $CoFe_2O_4$ nanoparticles. Using the microwave combustion method, $CoFe_2O_4$ nanoparticles synthesized from *Aloe vera* leaf extract had a surface area of 93 m^2 g^{-1} and an average particle size of 15 nm.[64] Meanwhile, Nimshi *et al.*[80] synthesized $CoFe_2O_4$ nanoparticles using *Pedalium murex* leaf extract *via* microwave irradiation, resulting in a surface area of 158 m^2 g^{-1} and an average particle size of 42 nm. Regardless of the type of plant extract used, a similar method (calcination or microwave assistance) and similar synthesis conditions (time and temperature) were employed, and an increase in surface area was generally observed as particle size increased.

On evaluating the effects of conventional heating and microwave-assisted methods on the synthesis of $CoFe_2O_4$ nanoparticles from *Aloe vera* leaf extract, the results showed the opposite trend, *i.e.*, the specific surface area of $CoFe_2O_4$ nanoparticles increases with the reduction in average particle size.[64] This phenomenon can be explained by the fact that during the high-temperature heating process above 500 °C in the conventional method, many capping agents in the plant extract decompose, leading to a lack of stabilizing agents and particle encapsulation (72 m^2 g^{-1}, 27 nm).[64] On the other hand, the microwave combustion method allowed $CoFe_2O_4$ nanoparticles to form with the help of *Aloe vera* leaf extract, where the capping agents remain intact, resulting in smaller particle sizes of 15 nm and a larger surface area (93 m^2 g^{-1}).[64] In summary, depending on the synthesis conditions, there are different trends in the surface area of green $CoFe_2O_4$ nanoparticles. Additionally, the role of phytochemicals in providing capping and stabilizing agents significantly influences the specific surface area of cobalt ferrite.

3.2. Particle size

The variation in cobalt ferrite grain size is highly correlated with the synthesis conditions and methods used. Table S1† demonstrates that changes in synthesis conditions, such as synthesis time, temperature, treatment method, and extract dosage, significantly impact the average size of cobalt ferrite nanoparticles. The data indicate that the amount of extract used and the calcination temperature during the synthesis of $CoFe_2O_4$ nanoparticles notably influence the particle size.

First, varying the amount of plant extract does not show a consistent trend in increasing or decreasing the average size of $CoFe_2O_4$ nanoparticles. For instance, Kavitha *et al.*[81] evaluated the average size of green $CoFe_2O_4$ nanoparticles by increasing the amount of *Erythrina variegata* leaf extract used in the synthesis. The results showed that increasing the extract volume from 10 to 40 mL decreased the average nanoparticle size from 38 to 30 nm.[81] Conversely, another study observed the opposite trend using verjuice extract; with the extract volume increasing from 10 to 40 mL, the average size of $CoFe_2O_4$ nanoparticles increased from 21 to 42 nm.[32] Even when examining a wider margin of verjuice extract amounts from 1 to 60 mL, the average nanoparticle size showed a random distribution with no clear trend.[32] Although the complexing and capping agents of plant extracts play a crucial role in the formation and stabilization of nanoparticles, the diversity of phytochemical components results in varied complexing interactions and encapsulation mechanisms. Therefore, determining the exact mechanism for nanoparticle formation from plant extracts remains controversial.

Besides the significant influence of the amount of extract used, the processing temperature during the synthesis of $CoFe_2O_4$ nanoparticles also plays an important role in determining particle size. The data indicate that when other synthesis factors are held constant, an increase in synthesis temperature results in larger $CoFe_2O_4$ nanoparticle size. For example, Miri *et al.*[82] synthesized $CoFe_2O_4$ nanoparticles from Torajabin plant extract at temperatures of 600, 700, and 800 °C. The average sizes of the nanoparticles were 27.7 nm at 600 °C, 44.3 nm at 700 °C, and 58.4 nm at 800 °C.[82] A similar trend was observed with $CoFe_2O_4$ nanoparticles synthesized from verjuice extract; the particle size increased from 14 nm at 600 °C to 21 nm at 700 °C, and 34 nm at 800 °C.[32] This trend is not limited to the green synthesis of $CoFe_2O_4$ nanoparticles. For example, Nitika *et al.*[83] demonstrated that using the coprecipitation method through chemical routes, the average size of $CoFe_2O_4$ nanoparticles increased from 22 nm to 42 nm since the calcination temperature was raised from 500 °C to 700 °C. This phenomenon can be explained by the decomposition of phytochemical molecules at high calcination temperatures, which reduces the availability of capping and stabilizing agents. Additionally, at high temperatures, the Brownian motion of $CoFe_2O_4$ molecules increases, causing them to move faster and collide more frequently. This heightened collision rate promotes agglomeration among $CoFe_2O_4$ molecules.[84] Consequently, $CoFe_2O_4$ nanoparticles tend to cluster together, leading to an increase in grain size at higher calcination temperatures.

3.3. Morphology

SEM and TEM images of $CoFe_2O_4$ nanoparticles provide an overview of their exterior structure, shape, surface roughness, degree of particle aggregation, and distribution of morphological types within a cluster (Fig. 3). These images reveal that spherical $CoFe_2O_4$ nanoparticles constitute over 74% of the samples studied. Other morphologies, such as cubic, polyhedral, flake-like, bipyramidal, and bud-like shapes, represent from 4% to 8% (Fig. 4). The shape of $CoFe_2O_4$ nanoparticles varies with synthesis parameters, including temperature, time, solvent, and the precursor ion-to-solvent ratio, as well as the physicochemical properties of the sample post-synthesis. Similarly, in the chemical synthesis route, the spherical forms of $CoFe_2O_4$ nanoparticles can be found in several previous reports.[85–87]

3.4. Band gap energy

Band gap energy measures the minimum energy required for the excitation phenomenon to occur, an important optical and electrochemical property of $CoFe_2O_4$ nanoparticles. Table S1† shows that the average band gap energy of green $CoFe_2O_4$

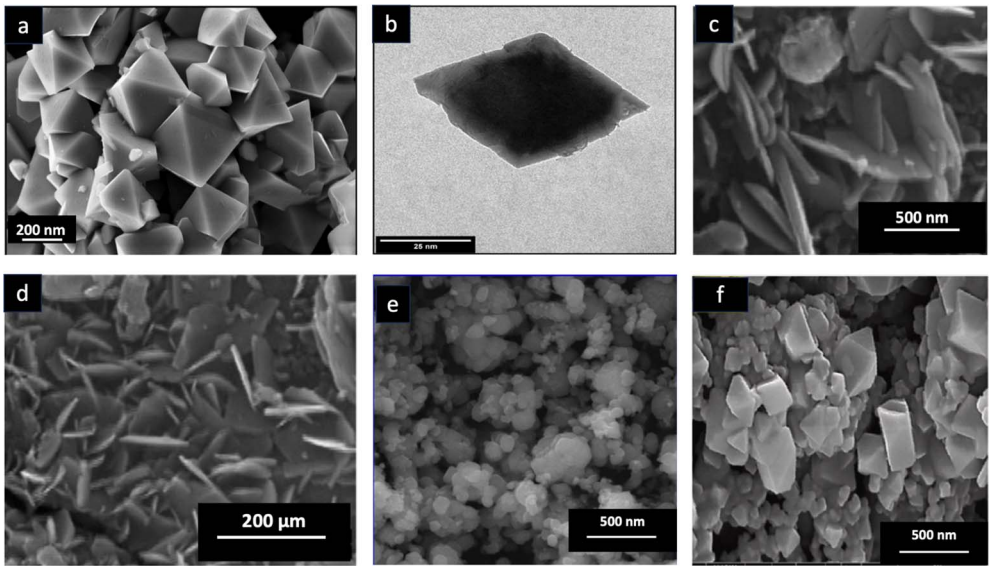

Fig. 3 (a) SEM image and (b) TEM image of the octahedral bipyramid structure of green $CoFe_2O_4$. Reproduced with the permission of MDPI from ref. 48 copyright 2022. (c) and (d) SEM images of the flake-like nanoplatelet structure of green $CoFe_2O_4$. Reproduced with the permission of Elsevier from ref. 64 copyright 2014. (e) SEM image of the spherical structure of green $CoFe_2O_4$. Reproduced with the permission of Elsevier from ref. 63 copyright 2017. (f) SEM image of the polyhedral structure of green $CoFe_2O_4$. Reproduced with the permission of Elsevier from ref. 32 copyright 2022.

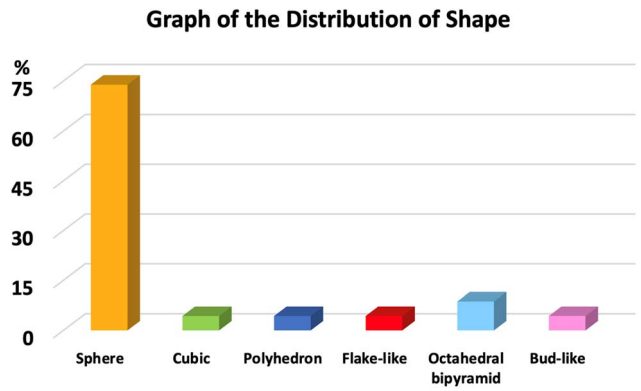

Fig. 4 The distribution of the shape of green cobalt ferrite nanoparticles. Note: data were collected from the relevant references cited in this work.

nanoparticles synthesized from plant extracts ranges from 1.36 eV to 4.5 eV. This variation is due to several factors in the synthesis process. First, different heating treatments influence the band gap energy. $CoFe_2O_4$ nanoparticles synthesized *via* microwave-assisted methods generally have lower band gap energies compared to those synthesized using traditional heating methods. For example, $CoFe_2O_4$ nanoparticles synthesized from *Hibiscus rosa-sinensis* flower extract using conventional heating at 1000 °C have a band gap energy of 2.06 eV, whereas those synthesized with microwave assistance have a band gap energy of 1.87 eV.[63] Similarly, $CoFe_2O_4$ nanoparticles synthesized from *Opuntia dillenii* haw extract using conventional combustion methods and microwave combustion methods have band gap energies of 2.01 eV and 1.93 eV, respectively.[78] This phenomenon can be explained as when the calcination temperature is raised, the absorption band in the UV-DRS shifts to a shorter wavelength. Increasing the calcination temperature raises the concentration of oxygen vacancies, shifting the absorption band to a shorter wavelength and widening the band gap in the conventional heating method. Ferrites typically have two band structures: the O-2p orbital as the valence band and the F-3d orbital as the conduction band. As a result, more energy is needed to excite electrons from the valence band (O-2p) to the conduction band.[88,89]

Furthermore, the type of extract used significantly affects the band gap energy of $CoFe_2O_4$ nanoparticles. Chandrani *et al.*[16] evaluated the band gap energy of $CoFe_2O_4$ nanoparticles synthesized from two different extracts. The results show that $CoFe_2O_4$ nanoparticles synthesized from *Zingiber officinale* root extract have a band gap energy of 1.44 eV, while those synthesized from *Elettaria cardamomum* seed extract have a band gap energy of 1.36 eV.[16] The different components in these plant extracts influence the complexation process and the formation of distinct crystal lattices, resulting in variations in lattice parameters and consequently, differences in band gap energy.[78]

3.5. Saturation magnetization

Saturation magnetization (M_S) refers to the highest magnetization achievable when an external magnetic field aligns with the easy magnetization axis of domains within a magnetic material.[90] The surface effect, or the dead surface, of magnetic materials is often linked to the disorder of surface spins.[91] An increase in the number of surface spins in a sample results in a decrease in saturation magnetization.[78] Besides surface spins, Kombaiah *et al.*[63] suggested that the synthesis process of

$CoFe_2O_4$ nanoparticles at high temperature tends to increase the saturation magnetization of green $CoFe_2O_4$ nanoparticles. Table S1† highlights a trend in calcination temperature affecting the saturation magnetization of $CoFe_2O_4$ nanoparticles in several reports. For example, Miri *et al.*[82] synthesized $CoFe_2O_4$ nanoparticles from Torajabin plant extract and demonstrated that increasing the temperature from 600 to 800 °C raised the saturation magnetization from 67 to 81 emu g^{-1}. This phenomenon is explained by the fact that higher calcination temperatures increase the crystalline size of the sample.[92] As the crystallite size increases, the number of surface spins in the sample decreases, leading to an increase in saturation magnetization.[78]

Furthermore, there is a link between particle size and saturation magnetization; the larger the particle size, the higher the saturation magnetization of green $CoFe_2O_4$ nanoparticles. Indeed, Miri *et al.*[82] showed a trend in particle size affecting the saturation magnetization of $CoFe_2O_4$ nanoparticles synthesized from Torajabin plant extract. Increasing the particle size from 27 to 58 nm led to a rise in saturation magnetization from 67 to 81 emu g^{-1}. This increase is attributed to the reduction in the surface-to-volume ratio associated with larger particle sizes, thereby increasing saturation magnetization. A similar trend in particle size and saturation magnetization was also observed in the synthesis of $CoFe_2O_4$ nanoparticles using the thermal decomposition method assisted by chemical solvents (oleylamine and dodecanediol).[93] In another report, Lamouri *et al.*[94] indicated a similar trend, where increasing particle size led to an increase in the saturation magnetization of $CoFe_2O_4$ hard ferrite nanoparticles.

Notably, the saturation magnetization of most green $CoFe_2O_4$ nanoparticles is lower than that of bulk $CoFe_2O_4$ (94 emu g^{-1}).[95] This phenomenon is due to the presence of atoms like potassium, calcium, and magnesium in the plant extract, which compete for and occupy octahedral positions, replacing Fe^{3+} ions with Fe^{2+} ions.[18,96] This replacement weakens the super-exchange interaction between magnetic atoms at octahedral and tetrahedral sites, leading to a reduction in the net magnetic moment.[18] The phenomenon of reduced saturation magnetization in green ferrite nanoparticles was also observed in $ZnFe_2O_4$ nanoparticles synthesized from plant extracts. The saturation magnetization of these $ZnFe_2O_4$ nanoparticles was less than 30 emu g^{-1}, whereas chemically synthesized $ZnFe_2O_4$ nanoparticles can achieve values between 30 and 60 emu g^{-1}.[10]

3.6. Crystallinity

Crystallinity of $ZnFe_2O_4$ nanoparticles can be analyzed using the X-ray diffraction (XRD) profile. Indeed, characteristic peaks are indexed for the (111), (220), (311), (222), (400), (422), (511), (440), (620), (533), (622), and (622) planes, corresponding to face-center-cubic (fcc) spinel ferrite structure (JCPDS no. 22-1086).[32,45,96] Moreover, there is no significant crystallite change in peak position between $CoFe_2O_4$ nanoparticles synthesized using chemical methods and green methods *via* plant extracts. This finding can be due to the fact that calcination at high temperatures results in the deconstruction of phytochemicals covered in the surface of $CoFe_2O_4$ nanoparticles. However, the change in XRD peak intensity can be dependent on the synthesis condition, *i.e.*, plant extract volume. For example, Kiani *et al.*[32] detected that increasing the verjuice extract volume from 10 mL to 50 mL decreased the peak intensity of biosynthesized $CoFe_2O_4$ nanoparticles and gradually formed the second phase of α-Fe_2O_3. By contrast, a very large amount of verjuice extract caused greater precipitation of the carboxylic acid–Fe complex, decreasing the purity of $CoFe_2O_4$ nanoparticles.

4. Applications of biosynthesized $CoFe_2O_4$ nanoparticles

4.1. Biomedical activity

4.1.1. Antimicrobial. Bacteria and fungi are microorganisms with a significant influence on the growth and development cycle of the entire biogeochemical cycle on the earth. These two groups play crucial roles in maintaining the stability of the food chain, with bacteria acting as key modulators of rapid carbon cycling pathways in soils, while fungi are primarily responsible for breaking down refractory organic matter.[97] Additionally, due to characteristics such as the ability to quickly generate biomass, low costs, and high profitability, many industrial production processes utilize bacterial and fungal communities, yielding great benefits for the food, biotechnology, and biomedical industries.[98] However, the impact of bacteria and fungi on agriculture and human health poses significant challenges. In agriculture alone, bacterial and fungal pathogens cause 20–40% of the total global food production losses each year.[99] Regarding human health, bacterial and fungal invasions can lead to various health issues, including self-limited pneumonia, blastomycosis, disseminated coccidioidomycosis, severe digestive problems, and the phenomenon of multidrug resistance among colonized microorganisms.[100–102] To combat these harmful microorganisms, metal and metallic oxide nanoparticles have recently become preferred materials due to their cytotoxic properties to produce reactive oxygen species to kill bacteria and fungi.[103]

Thanks to their cytotoxic properties and favorable physicochemical characteristics (such as nano size and low band gap), $CoFe_2O_4$ and $CoFe_2O_4$-based nanocomposites are considered potential tools for killing harmful bacteria.[23] Table S2† demonstrates that green $CoFe_2O_4$ and $CoFe_2O_4$-based nanocomposites can effectively kill a variety of bacterial strains, both Gram-negative and Gram-positive, as well as multidrug-resistant strains. These findings are supported by methods such as inhibition zone, MIC (minimum inhibitory concentration), and MBC (minimum bactericidal concentration). For example, Ansari *et al.*[8] showed that $CoFe_2O_4$ nanoparticles synthesized from *Aloe vera* leaf extract have MICs of 0.25 mg mL^{-1} against multidrug-resistant *Pseudomonas aeruginosa*. Additionally, Gingasu *et al.*[62] reported that the MIC value for Gram-positive *Enterococcus faecalis* can reach as low as 0.062 mg mL^{-1}. Moreover, the antibacterial performance of green $CoFe_2O_4$ nanoparticles is comparable to those synthesized by

other physicochemical methods. Palanisamy *et al.*[104] and Kalia *et al.*[105] demonstrated the effectiveness of $CoFe_2O_4$ nanoparticles synthesized by sol–gel and wet precipitation methods in treating bacteria of the *Bacillus* and *Coccus* families, with inhibition zone values ranging from 6 to 8.5 mm. In comparison, the inhibition zones of green $CoFe_2O_4$ nanoparticles, as shown in Table S2,† range from approximately 6 to 12 mm. These results highlight the antibacterial potential of $CoFe_2O_4$ nanoparticles synthesized from plant extracts, making them suitable for treating various bacterial strains. However, their performance can be further enhanced by doping with other antibacterial active materials.

The database shows that $CoFe_2O_4$ nanoparticles doped with Ag or graphite materials significantly enhance the performance in killing all types of bacteria. For example, $CoFe_2O_4$ nanoparticles synthesized from *Carissa carandas* plant extracts were found to inhibit *Staphylococcus aureus* and *Escherichia coli* with inhibition zones of 12 mm and 14 mm, respectively.[19] In contrast, Ag/$CoFe_2O_4$ nanocomposites synthesized from *Carissa carandas* extracts showed inhibition zones for *Staphylococcus aureus* and *Escherichia coli* ranging from 17 mm to 19 mm, respectively.[19] Furthermore, the MIC against *Pseudomonas aeruginosa* strains was significantly lower for Ag/$CoFe_2O_4$ nanocomposites synthesized from *Moringa oleifera* gum (0.028 mg mL^{-1}) compared to $CoFe_2O_4$ nanoparticles from *Moringa oleifera* gum (0.139 mg mL^{-1}).[49] This enhancement is attributed to the excellent antibacterial properties of Ag, which have been well-documented in previous reports. By combining with $CoFe_2O_4$ nanoparticles, the Ag/$CoFe_2O_4$ nanocomposite exhibits increased antibacterial activity without losing the intrinsic antibacterial properties of $CoFe_2O_4$ nanoparticles.[19] However, the process of doping Ag onto $CoFe_2O_4$ nanoparticles needs to be carefully evaluated and optimized to achieve the highest bacterial treatment efficiency and to optimize the cost of the Ag used.

Additionally, plant extract-derived $CoFe_2O_4$ nanoparticles exhibit significant antifungal activity. Beyond their antibacterial properties, $CoFe_2O_4$ nanoparticles show potential for killing various types of fungi, such as *Aspergillus aureus*, *Candida krusei*, *Candida albicans*, and *Candida parapsilosis*. The inhibition zones for these fungal strains range from 8.5 to 15 mm, with MIC values between 0.75 and 1 mg mL^{-1} (Table S2†). However, a limitation in investigating the antifungal activity of green $CoFe_2O_4$ nanoparticles is the lack of studies evaluating the effects of green $CoFe_2O_4$ hybrid composites. Consequently, there is a limited database for comparing the antifungal effectiveness of green $CoFe_2O_4$ with other composite hybrids. Despite this, the strong antibacterial and antifungal potential of green $CoFe_2O_4$ nanoparticle-based materials suggests promising opportunities for scaling up industrial production for biomedical applications.

In general, the effectiveness of $CoFe_2O_4$ nanoparticles in antifungal and antibacterial activity is attributed to two main mechanisms: apoptosis and reactive oxygen species (ROS) process. The high efficiency of $CoFe_2O_4$ nanoparticles in antimicrobial activity is attributed to their cytotoxicity, which induces the apoptosis process. They generate reactive oxygen species to attack the cell walls and internal structures of microorganisms. Thanks to their small particle size and high biocompatibility, $CoFe_2O_4$ nanoparticles can penetrate the cell membrane, causing cell apoptosis and leading to microbial death.[43] In addition to inducing apoptosis, the formation of reactive oxygen species by $CoFe_2O_4$ nanoparticles is also responsible for effectively treating microorganisms (Fig. 5). In this mechanism, reactive oxygen species act as free radicals that attack cell walls, causing rupture and cytoplasmic leakage, and damage DNA, mitochondria, and proteins, ultimately leading to the death of microorganisms.[106] The formation of reactive oxygen species occurs when the energy from an irradiated photon source is absorbed by the material, leading to electron excitation to the conduction band and hole formation in the valence band. These electrons and holes interact with molecules such as oxygen and water in the medium, creating free radicals such as $^{\bullet}OH$ and $O_2^{\bullet -}$. These free radicals then attack and destroy microorganisms.

4.1.2. Anticancer activity. Cytotoxicity is a crucial factor that strongly impacts the effectiveness of the anticancer activity of $CoFe_2O_4$ nanoparticles. The results from Table S2† show the strong anticancer ability of green $CoFe_2O_4$ nanoparticle-derived agents on multiple cancer cell lines. *In vitro* experimental models on colon cancer cells ($CaCo_2$) and a healthy cell line of mouse embryo fibroblast were used to evaluate this effect. Miri *et al.*[82] showed that, in addition to being cytotoxic, green $CoFe_2O_4$ nanoparticles synthesized from Torajabin extract can target cancer cells while avoiding harm to healthy cells. The dose needed to achieve a 50% inhibition concentration (IC_{50}) with $CaCo_2$ cells is 1095 μg mL^{-1}, whereas for the healthy mouse embryo fibroblast cell line, this value is more than double (2502 μg mL^{-1}). Notably, the anticancer effectiveness of $CoFe_2O_4$ nanoparticles is significantly improved as they are combined with Ag nanoparticles. Specifically, to inhibit 50% of human breast cancer MCF-7 cell lines, the dose of Torajabin extract-synthesized $CoFe_2O_4$ nanoparticles is 1811 μg mL^{-1}.[82] In contrast, green $CoFe_2O_4$/Ag nanoparticles require only 60 μg mL^{-1} to achieve the same effect.[19] The ability to induce cytotoxicity, target harmful cell lines, maintain biocompatibility, and combine effectively with enhancing materials makes $CoFe_2O_4$ nanoparticles a priority for anticancer activities. However, the potential of $CoFe_2O_4$ nanoparticles in the

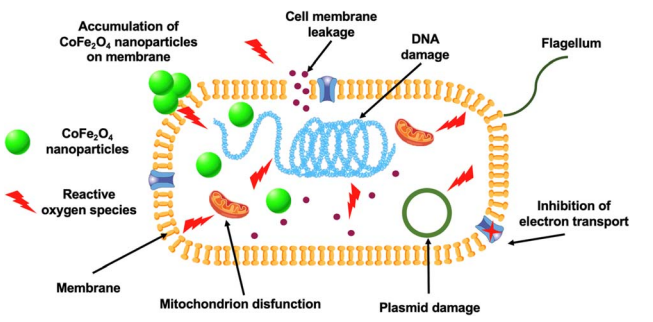

Fig. 5 Formation mechanism of reactive oxygen species for bacteria killing by cobalt ferrite nanoparticles.

anticancer field is not limited to cytotoxicity alone; they can also act through the hyperthermia mechanism. Unfortunately, the anticancer effectiveness of hyperthermia treatment using green $CoFe_2O_4$ nanoparticles has not been widely evaluated. Therefore, it is essential to investigate the hyperthermia treatment potential of green $CoFe_2O_4$ nanoparticles to provide a basis for comparing anticancer activity in *in vivo* and *in vitro* models.

The anticancer potential of $CoFe_2O_4$ nanoparticles against multiple cancer cell lines through hyperthermia treatment is substantial. However, the use of plant extract-synthesized $CoFe_2O_4$ nanoparticles for cancer treatment *via* hyperthermia is still limited. Studies have shown that these $CoFe_2O_4$ nanoparticles are effective in treating various cancer cell lines, such as human epidermoid carcinoma (A431), breast cancer (MCF-7), and B16 melanoma (human skin cancer).[107–109] Some preliminary studies to evaluate the hyperthermia treatment potential of plant extract-synthesized $CoFe_2O_4$ nanoparticles have also shown positive results. For instance, assessing the ability of *Aloe vera* leaf extract-synthesized $CoFe_2O_4$ nanoparticles to generate heat under an alternating magnetic field, Hermosa *et al.*[65] demonstrated that these nanoparticles could increase the temperature to 42 °C in 15 min, with a specific absorption rate (SAR) value of 107 W g^{-1}. These parameters indicate that the anticancer potential of green $CoFe_2O_4$ nanoparticles through hyperthermia treatment is feasible and promising. Indeed, when $CoFe_2O_4$ nanoparticles are placed under an alternating magnetic field, they undergo Néel and Brownian relaxation, generating heat (41–43 °C).[110] At this temperature, cancer cells are destroyed due to poor blood flow and insufficient oxygen, while normal cells remain unharmed, as surrounding tissues are damaged at temperatures above 46 °C.[42] The specific absorption rate quantifies the heat power generated per unit mass of magnetic nanoferrite per unit time, directly reflecting the function of magnetic nanoferrite in heating and treating tumor cells. The SAR value of *Aloe vera* leaf extract-synthesized $CoFe_2O_4$ (107 W g^{-1}) showed comparable performance with some reports of Hatamie *et al.*[108] and Fantechi *et al.*[107] though it is still lower than the SAR values reported for other $CoFe_2O_4$ nanoparticles, such as 200 W g^{-1} of Balakrishnan *et al.*[109] and 150 W g^{-1} of Nandhini and Shobana.[111] Despite this, the SAR value is still considered significant for treating tumor cells, and the potential anticancer activity of *Aloe vera* leaf extract-synthesized $CoFe_2O_4$ is highly recommended.[65]

There are, however, still some issues that remain regarding hyperthermia treatment with magnetic ceramide nanocomposites. Hyperthermia treatment must be precisely controlled to ensure that only the targeted tumor tissue is heated, as it relies on hysteresis heat loss.[111] Additionally, the mechanism of hyperthermia-induced cytotoxicity in tumor cells is not yet fully understood.[111] Consequently, applying hyperthermia treatment of $CoFe_2O_4$ nanoparticles in in-depth tests and *in vivo* experiments faces several limitations. Despite these challenges, the potential hyperthermia treatment of plant extract-synthesized $CoFe_2O_4$ nanoparticles should be thoroughly evaluated and investigated to supplement the existing database on the biomedical activities of green $CoFe_2O_4$ nanoparticles. This research could open up broad application possibilities for green $CoFe_2O_4$ nanoparticles in cancer treatment and other biomedical fields.

4.2. Water treatment

4.2.1. Organic dyes. Recently, the photocatalytic activity of $CoFe_2O_4$ nanoparticles in the photodegradation of organic dyes has shown good efficiency in treating various organic dye pollutants in water. This is attributed to their low band gap energy (1.36 eV to 4.5 eV), which allows $CoFe_2O_4$ nanoparticle-based materials to be easily excited by photon sources from UV and visible light. Indeed, Kavitha *et al.*[81] conducted photodegradation studies of crystal violet and Congo red dyes using $CoFe_2O_4$ nanoparticles synthesized from *Erythrina variegata* leaf extract. The results showed that the photodegradation efficiency of these green $CoFe_2O_4$ nanoparticles was 85% for crystal violet and 79% for Congo red under visible light.[81] Additionally, the same photon source was used by the author to demonstrate that $CoFe_2O_4$ nanoparticles synthesized from *Hibiscus rosa-sinensis* leaves achieved 84% photodegradation efficiency with methylene blue.[47] The good physical performance of these green $CoFe_2O_4$ nanoparticles with multiple organic dyes is attributed to their low band gap energy. At this energy level, the $CoFe_2O_4$ nanoparticle-based catalyst is easily excited by photon energy in the visible region, enhancing their catalytic activity.

In addition to band gap energy, differences in plant extracts used in the synthesis of $CoFe_2O_4$ nanoparticles also lead to variations in dye treatment efficiency. For example, Chandrani *et al.*[16] evaluated the effectiveness of $CoFe_2O_4$ nanoparticles derived from ginger root extract and cardamom seed extract in treating phenol red. The results showed that, despite identical synthesis and experimental conditions as well as an energy band gap of approximately 1.4 eV for both types of green $CoFe_2O_4$ nanoparticles, the treatment effectiveness for phenol red was 91% with ginger root extract-derived $CoFe_2O_4$ nanoparticles and 75% with cardamom seed extract-derived $CoFe_2O_4$ nanoparticles.[16] This phenomenon can be explained by the differences in the types of plant extracts used for synthesis. The varying phytochemical components in each type of extract lead to differences in the chelation and stabilization processes, resulting in different properties of the green $CoFe_2O_4$ nanoparticles. This variability is a limitation of the green synthesis method, as the materials obtained often exhibit low stability and application efficiency compared to those synthesized by physical and chemical methods.

To enhance the photodegradation efficiency of green $CoFe_2O_4$ nanoparticles with organic dyes, combined processes involving materials such as CeO_2, ZnO, Ag, and graphene oxide have been utilized. These combinations aim to reduce the band gap of green $CoFe_2O_4$ nanoparticle-based nanocomposites while facilitating the excitation process. For instance, to improve the rhodamine B photodegradation efficiency of $CoFe_2O_4$ nanoparticles synthesized from *Carissa carandas* bark extract (approximately 78%), Punyasamudram *et al.*[19] successfully synthesized $CoFe_2O_4$@Ag nanocomposites from *Carissa carandas* bark extract, achieving a degradation efficiency of over 97%. Similarly, Puspitarum *et al.*[112] investigated the effects of

$CoFe_2O_4$ nanoparticles and $CoFe_2O_4/TiO_2$ nanocomposites synthesized from *Moringa oleifera* leaf extract on the photodegradation of methylene blue, with effective removal rates of 61% and 99%, respectively. The superior decomposition efficiency of the $CoFe_2O_4$ nanocomposite can be attributed to the difference in energy band gaps between the two components in the composite, leading to a synergistic two-path mechanism.[19] More specifically, electrons in the elements move from the valence band to the conduction band upon excitation by a photon source. Then, electrons in the conduction band of one element move to the conduction band of the other element, depending on the degree of negative charge in the conduction bands. As a result, electrons in the conduction band and holes in the valence band interact with molecules such as O_2 or H_2O in solution, creating reactive oxygen species that directly decompose organic dyes.

The mechanism of organic dye decomposition by $CoFe_2O_4$ nanoparticles *via* the excitation process is illustrated in Fig. 6. More specifically, upon receiving photon irradiation from UV-visible light, electrons are excited to the conduction band, and holes appear in the valence band. These electron–hole pairs then interact with O_2 and H_2O molecules in the environment to form reactive oxygen species ($^{\bullet}O_2^-$ and $^{\bullet}OH$). These reactive oxygen species attack dye molecules in the water, decomposing them into degradation products such as CO_2 and H_2O. Besides that, to maintain the excitation process and prevent recombination, researchers have combined two semiconductors to create new heterojunction types, leading to a variety of photocatalytic mechanisms.[113] This has resulted in differences in the photocatalytic activity and dye treatment efficiency of some $CoFe_2O_4$ nanocomposites (Table S3†).

In addition to their ability to treat molecular dyes through a photodegradation catalytic mechanism, the adsorption capacity of green $CoFe_2O_4$ nanoparticles for organic dyes has also shown high potential in treating organic dyes. Liaskovska *et al.*[114] evaluated the adsorption efficiency of Congo red using $CoFe_2O_4$ nanoparticles synthesized from *Ginkgo biloba* leaf extract. The results showed that the adsorption capacity of green $CoFe_2O_4$ nanoparticles is 45.7 mg g^{-1}. This adsorption efficiency is attributed to the good electrostatic interaction between the positively charged surface of $CoFe_2O_4$ nanoparticles and Congo red anionic dyes, following the donor–acceptor mechanism.[114] This result is also relatively positive compared to $CoFe_2O_4$ nanoparticles synthesized by chemical methods. Olusegun and Mohallem,[115] and Cao *et al.*[116] reported that chemically synthesized $CoFe_2O_4$ nanoparticles had adsorption capacities of approximately 50–70 mg g^{-1}. Although the adsorption efficiency of green $CoFe_2O_4$ nanoparticles is somewhat lower than that of their chemically synthesized counterparts, the convenience and safety of the synthesis process make $CoFe_2O_4$ nanoparticles synthesized from plant extracts a viable alternative to traditional synthetic nanomaterials.

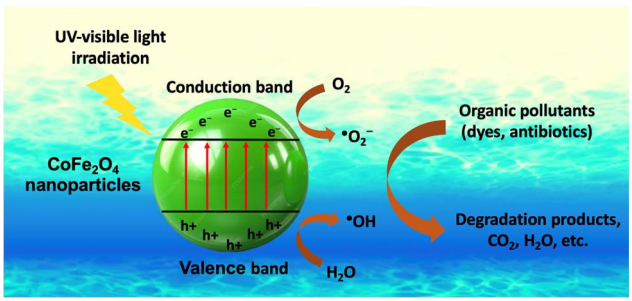

Fig. 6 The formation mechanism of reactive oxygen species for the degradation of organic pollutants by cobalt ferrite nanoparticles.

4.2.2. Heavy metal ions. The performance of green $CoFe_2O_4$ nanoparticles not only shows great efficiency with dyes but also with heavy metal ions such as Pb^{2+}. Indeed, Tasqeen *et al.*[117] demonstrated that Ag–$CoFe_2O_4$ nanocomposites synthesized from *Taxus wallichiana* leaf extract have a Pb^{2+} adsorption capacity of up to 33.0 mg g^{-1}. The excellent Pb^{2+} adsorption efficiency of the Ag–$CoFe_2O_4$ nanocomposite is attributed to the rich chemical surface of functional groups derived from the plant extract. These functional groups interact with Pb^{2+} ions to form bonds such as Pb–O and Pb–O–Pb, which are observed through the FTIR spectrum with peaks at 462 and 686 cm^{-1}, respectively.[117] However, there are currently fewer reports regarding the adsorption potential of plant extract-synthesized $CoFe_2O_4$ nanoparticles on heavy metals. Therefore, further research on the adsorption of heavy metals by green $CoFe_2O_4$ nanoparticles is called for. Additionally, accurately evaluating the mechanisms occurring in the heavy metal adsorption process through comprehensive analyses such as X-ray photoelectron spectroscopy (XPS) and FTIR is essential. Future studies should focus on enhancing the heavy metal adsorption efficiency by modifying green $CoFe_2O_4$ nanoparticles with materials that have large surface areas, such as activated carbon, bacterial cellulose, and polymers. This could lead to the development of composites with increased adsorption efficiency. Finally, the economic feasibility of using green $CoFe_2O_4$ nanoparticles in the heavy metal adsorption process should be evaluated through reuse experiments to assess their stability and suitability for practical applications.

4.2.3. Pharmaceutical drugs. Besides the ability to treat a variety of dyes and heavy metals, $CoFe_2O_4$-based composites also show potential in treating a variety of antibiotics, such as tetracycline, ciprofloxacin, and paracetamol. Through a photodegradation path, Oliveira *et al.*[118] demonstrated that green $CoFe_2O_4$@Nb_2O_5 synthesized from tangerine peel extract effectively catalyses the paracetamol decomposition, achieving more than 97% degradation under UV-visible light after 60 min. Notably, recent studies have designed antibiotic decomposition models that combine ultrasound support to increase the effectiveness of antibiotic decomposition. For example, Nimshi *et al.*[80] evaluated the effectiveness of decomposing tetracycline and ciprofloxacin using $CoFe_2O_4$@TiO_2@reduced graphene oxide synthesized from *Pedalium murex* leaf extract, employing three decomposition pathways: sonocatalytic, photocatalytic, and sonophotocatalytic. The results showed that the sonophotocatalytic pathway was the most effective, with degradation efficiencies of 92% for tetracycline and 84% for ciprofloxacin. In contrast, the photocatalytic pathway achieved 70% and 47%

degradation, and the sonocatalytic pathway achieved 40% and 26%, respectively. This trend is explained by the fact that ultrasound increases the chaotic density of particles (antibiotic and catalyst) in the solution, reducing particle agglomeration, increasing the frequent collision between antibiotic molecules and catalyst particles. This provides antibiotic molecules easier access to the active centers of catalysis, due to the synergy between ultrasound and photon sources and thereby increasing the efficiency of antibiotic decomposition. Furthermore, Nimshi *et al.*[80] also investigated the reuse potential and found that the photodegradation efficiency of the green $CoFe_2O_4$ nanocomposite remained stable after five rounds of reuse. These reports demonstrate the strong antibiotic-degrading ability and recyclability of green $CoFe_2O_4$ nanoparticle-based nanocomposites, indicating potential for large-scale antibiotic treatment with high economic viability in the future.

5. Future prospects and limitations

5.1. Future prospects

This review highlights the promising future prospects for the application of $CoFe_2O_4$ nanoparticles synthesized from plant extracts in addressing water treatment and biomedical challenges. Additionally, the environmental advantages of the green synthesis method for $CoFe_2O_4$ nanoparticles make it a more eco-friendly alternative to traditional synthesis methods. The use of phytochemicals as complexing, capping, and stabilizing agents replaces chemical solvents, supporting the successful synthesis of green $CoFe_2O_4$ nanoparticles. Studies have shown that the optical and magnetic properties of green $CoFe_2O_4$ nanoparticles are comparable to those synthesized using conventional methods. These characteristics such as low band gap, great magnetic features, and nanosize of green $CoFe_2O_4$ nanoparticles are key factors in the high efficiency of green $CoFe_2O_4$ nanoparticles in achieving desired outcomes.

- Recently, several reports have investigated the applicability of plant extract-derived $CoFe_2O_4$ nanoparticles in fields such as cell energy, capacitors, sensors, and detectors.[18,48,69,73,77] This expansion broadens the application spectrum of green $CoFe_2O_4$ nanoparticles, enhancing their utility.

- Another advantage of the green synthesis of $CoFe_2O_4$ nanoparticles from plant extracts is the ability to use agricultural waste, such as peels, leaves, and branches, in the production process. This capability supports the industrial production of green $CoFe_2O_4$ nanoparticles as an important component in the circular economy.

Overall, due to these advantages, robust research and development of green $CoFe_2O_4$ nanoparticles should be pursued to maximize their production and application potential. This will contribute to sustainable global development.

5.2. Limitation aspects

Some remaining limitations in the synthesis of green $CoFe_2O_4$ nanoparticles significantly affect the strong development prospects of this material:

- Although plant extracts used for synthesis can replace toxic chemical solvents, the residual waste after the extraction process can cause secondary pollution. Therefore, measures are needed to address these waste residues, such as using them as biofertilizers, converting them into biochar or activated carbon, or producing other valuable biological products.

- The studies only highlight a few efforts to develop hybrid composites between green $CoFe_2O_4$ nanoparticles and reinforcement materials. This limitation has reduced the exploration of intrinsic properties and potential applications of green $CoFe_2O_4$-based composites.

- The use of green $CoFe_2O_4$ nanoparticles for water treatment applications also needs to consider the potential risk of releasing cobalt ions into the environment, as well as the incomplete recovery of cobalt ferrite nanoparticles. This may cause serious human health problems, such as anemia, fibrosis in the lungs, asthma, and peripheral neuropathy.[119,120]

- Additionally, regeneration experiments in wastewater treatment should be conducted to confirm the economic potential for industrial-scale production. The current reports primarily show the results of treating targets in the first round but do not provide much information about the effectiveness in subsequent rounds. This lack of data makes it difficult to determine whether green $CoFe_2O_4$ nanoparticles can ensure economic sustainability.

- The application of plant extract-synthesized $CoFe_2O_4$ nanocomposites in hyperthermia treatment for cancer also requires further study through *in vivo* experiments to evaluate the feasibility of these methods.

- To enhance the application potential of green $CoFe_2O_4$ nanocomposites in biomedicine fields, the cytotoxicity mechanism should be evaluated more accurately to ensure consistency between studies and to identify the most accurate proposed mechanism.

- Finally, several aspects of the synthesis and applications of biosynthesized $CoFe_2O_4$ in the fields of energy and catalysis may show potential, but are still not comprehensively explored. It is suggested that the exploration of this field should be strengthened in future studies.

Overall, while there is great potential in the production and application of green $CoFe_2O_4$ nanoparticles, the production process must address immediate obstacles to achieve greater developments in this field.

6. Conclusion

The biosynthesis of $CoFe_2O_4$ nanoparticles using plant extracts has represented a significant advancement in sustainable nanotechnology. This approach not only reduces reliance on toxic chemicals but also leverages the abundant and renewable resources found in plant materials. The resulting nanoparticles exhibit desirable properties, including high surface area, optimal particle size, unique morphology, suitable band gap energy, and notable saturation magnetization. They demonstrated effectiveness in biomedical applications, such as antimicrobial and anticancer treatments, as well as in environmental remediation, particularly water purification.

Despite challenges related to scalability and reproducibility, ongoing research should focus on optimizing synthesis protocols and exploring broader applications. This review highlights a promising future of plant extract-mediated nanoparticle synthesis to address critical environmental and health-related issues, thereby paving the way for more sustainable and efficient technologies.

Data availability

The data supporting this article have been included as part of the ESI.†

Author contributions

Giang Thanh Tran contributed to writing – original draft, investigation, methodology. Luan Minh Nguyen contributed to methodology, data curation. Thuy Thi Thanh Nguyen contributed to writing – review & editing, visualization. Dai Hai Nguyen contributed to writing – review & editing, validation. Thuan Van Tran contributed to conceptualization, writing – review & editing, supervision, project administration.

Conflicts of interest

The authors declare no conflict of interest.

Acknowledgements

This work is funded by the Foundation for Science and Technology Development Nguyen Tat Thanh University, Vietnam.

References

1 T. A. Wani and G. Suresh, *Adv. Sustainable Syst.*, 2022, **6**, 2200035.
2 S. Y. Srinivasan, K. M. Paknikar, D. Bodas and V. Gajbhiye, *Nanomedicine*, 2018, **13**, 1221–1238.
3 K. Wei, H.-X. Huai, B. Zhao, J. Zheng, G.-Q. Gao, X.-Y. Zheng and C.-C. Wang, *Sens. Actuators, B*, 2022, **369**, 132279.
4 C. Zhang, C. Ma, W. Zhang, Y. Wang, Z. U. Rehman, X. Shen and S. Yao, *Chem. Eng. J.*, 2024, **481**, 148374.
5 J. Liu, R. Meng, J. Li, P. Jian, L. Wang and R. Jian, *Appl. Catal., B*, 2019, **254**, 214–222.
6 B. A. Omran and K.-H. Baek, *J. Environ. Chem. Eng.*, 2023, **11**, 111465.
7 V. S. Coker, N. D. Telling, G. van der Laan, R. A. D. Pattrick, C. I. Pearce, E. Arenholz, F. Tuna, R. E. P. Winpenny and J. R. Lloyd, *ACS Nano*, 2009, **3**, 1922–1928.
8 M. A. Ansari, R. Govindasamy, M. Y. Begum, M. Ghazwani, A. Alqahtani, M. N. Alomary, Y. F. Jamous, S. A. Alyahya, S. Asiri, F. A. Khan, M. A. Almessiere and A. Baykal, *Nanotechnol. Rev.*, 2023, **12**, 20230575.
9 A. Manohar, V. Vijayakanth, S. V. P. Vattikuti and K. H. Kim, *Mater. Chem. Phys.*, 2022, **286**, 126117.
10 N. T. T. Nguyen, T. T. T. Nguyen, D. T. C. Nguyen and T. Van Tran, *Sci. Total Environ.*, 2023, **872**, 162212.
11 J.-L. Ortiz-Quiñonez, S. Das and U. Pal, *Prog. Mater. Sci.*, 2022, **130**, 100995.
12 A. Soufi, H. Hajjaoui, R. Elmoubarki, M. Abdennouri, S. Qourzal and N. Barka, *Appl. Surf. Sci. Adv.*, 2021, **6**, 100145.
13 F. Sharifianjazi, M. Moradi, N. Parvin, A. Nemati, A. J. Rad, N. Sheysi, A. Abouchenari, A. Mohammadi, S. Karbasi, Z. Ahmadi, A. Esmaeilkhanian, M. Irani, A. Pakseresht, S. Sahmani and M. Shahedi Asl, *Ceram. Int.*, 2020, **46**, 18391–18412.
14 A. S. Vijayanandan and R. M. Balakrishnan, *Appl. Phys. A*, 2020, **126**, 234.
15 E.-S. R. El-Sayed, H. K. Abdelhakim and Z. Zakaria, *Mater. Sci. Eng., C*, 2020, **107**, 110318.
16 D. N. Chandrani, S. Ghosh and A. R. Tanna, *J. Inorg. Organomet. Polym. Mater.*, 2024, **34**(7), 3100–3114.
17 D. A. Larasati, D. L. Puspitarum, M. Y. Darmawan, N. I. Istiqomah, J. Partini, H. Aliah and E. Suharyadi, *Results Mater.*, 2023, **19**, 100431.
18 A. Cheraghi, F. Davar, M. Homayoonfal and A. Hojjati-Najafabadi, *Ceram. Int.*, 2021, **47**, 20210–20219.
19 S. Punyasamudram, R. P. Puthalapattu, A. Bathinapatla, R. Mulpuri, S. Kanchi and P. V. N. Kumar, *Chemosphere*, 2024, **349**, 140892.
20 S. M. Ansari, K. C. Ghosh, R. S. Devan, D. Sen, P. U. Sastry, Y. D. Kolekar and C. V. Ramana, *ACS Omega*, 2020, **5**, 19315–19330.
21 M. I. Din, F. Rafique, M. S. Hussain, H. A. Mehmood and S. Waseem, *Sci. Prog.*, 2019, **102**, 61–72.
22 T. V. Sheena and J. Jacob, *Inorg. Chem. Commun.*, 2024, **167**, 112709.
23 F. Ameen and N. Majrashi, *Inorg. Chem. Commun.*, 2023, **156**, 111187.
24 M. Barani, A. Rahdar, M. Mukhtar, S. Razzaq, M. Qindeel, S. A. H. Olam, A. C. Paiva-Santos, N. Ajalli, S. Sargazi, D. Balakrishnan, A. K. Gupta and S. Pandey, *Mater. Today Chem.*, 2022, **26**, 101131.
25 Sonu, V. Dutta, S. Sharma, P. Raizada, A. Hosseini-Bandegharaei, V. K. Gupta and P. Singh, *J. Saudi Chem. Soc.*, 2019, **23**, 1119–1136.
26 G. Katoch, Himanshi, R. Jasrotia, J. Prakash, A. Verma, A. Kandwal, S. K. Godara, R. Verma, V. Raja and G. Kumar, *Mater. Today: Proc.*, 2023, DOI: **10.1016/j.matpr.2023.03.585**.
27 C. T. A. Xuan, P. T. Tho, N. D. Xuan, T. A. Ho, P. T. V. Ha, L. T. Q. Trang, N. Q. Tuan, D. H. Manh, T. D. Thanh and N. Tran, *J. Alloys Compd.*, 2024, **990**, 174429.
28 F. Ahmad and Y. Zhou, *Chem. Res. Toxicol.*, 2017, **30**, 492–507.
29 S. Kalia, A. Kumar, S. Sharma and N. Prasad, *J. Phys.: Conf. Ser.*, 2022, **2267**, 012133.
30 P. A. Vinosha, A. Manikandan, A. S. J. Ceicilia, A. Dinesh, G. F. Nirmala, A. C. Preetha, Y. Slimani, M. A. Almessiere, A. Baykal and B. Xavier, *Ceram. Int.*, 2021, **47**, 10512–10535.
31 S. Amiri and H. Shokrollahi, *Mater. Sci. Eng., C*, 2013, **33**, 1–8.

32 A. Kiani, F. Davar and M. Bazarganipour, *Ceram. Int.*, 2022, **48**, 34895–34906.
33 S. B. F. Santos, P. M. A. G. de Araújo, I. A. dos Santos, A. C. F. de M. Costa, Á. S. Lima and L. de S. Conrado, *Ceram. Int.*, 2021, **47**, 19622–19631.
34 S. Khizar, N. M. Ahmad, N. Ahmed, S. Manzoor, M. A. Hamayun, N. Naseer, M. K. L. Tenório, N. Lebaz and A. Elaissari, *Nanomaterials*, 2020, **10**, 2182.
35 D. Gheidari, M. Mehrdad, S. Maleki and S. Hosseini, *Heliyon*, 2020, **6**, e05058.
36 M. Suleman and S. Riaz, *J. Magn. Magn. Mater.*, 2020, **498**, 166143.
37 K. T. V. Oanh, H. T. L. Phong, D. N. Van, T. T. M. Trang, P. H. Thu, X. N. Truong, X. N. Ca, C. D. Linh, H. P. Nam and H. D. Manh, *J. Nanopart. Res.*, 2023, **25**, 212.
38 V. Mahdikhah, A. Ataie, A. Babaei, S. Sheibani, C. W. Ow-Yang and S. K. Abkenar, *Ceram. Int.*, 2020, **46**, 17903–17916.
39 J. Wang, B. Xiong, L. Miao, S. Wang, P. Xie, Z. Wang and J. Ma, *Appl. Catal., B*, 2021, **280**, 119422.
40 T. L. Lambat, P. V. Ledade, J. K. Gunjate, V. R. Bahekar, S. H. Mahmood and S. Banerjee, *Results Chem.*, 2023, **6**, 101176.
41 J. L. Ortiz-Quiñonez, S. Das and U. Pal, *Prog. Mater. Sci.*, 2022, **130**, 100995.
42 N. Akhlaghi and G. Najafpour-Darzi, *J. Ind. Eng. Chem.*, 2021, **103**, 292–304.
43 O. K. Mmelesi, N. Masunga, A. Kuvarega, T. T. Nkambule, B. B. Mamba and K. K. Kefeni, *Mater. Sci. Semicond. Process.*, 2021, **123**, 105523.
44 K. K. Kefeni, B. B. Mamba and T. A. M. Msagati, *Sep. Purif. Technol.*, 2017, **188**, 399–422.
45 K. Kombaiah, J. J. Vijaya, L. J. Kennedy, M. Bououdina, R. J. Ramalingam and H. A. Al-Lohedan, *Mater. Chem. Phys.*, 2018, **204**, 410–419.
46 P. A. Vinosha, A. Manikandan, A. C. Preetha, A. Dinesh, Y. Slimani, M. A. Almessiere, A. Baykal, B. Xavier and G. F. Nirmala, *J. Supercond. Novel Magn.*, 2021, **34**, 995–1018.
47 L. Velayutham, C. Parvathiraja, D. C. Anitha, K. Mahalakshmi, M. Jenila, F. A. Alasmary, A. S. Almalki, A. Iqbal and W.-C. Lai, *Nanomaterials*, 2022, **12**, 3668.
48 W. Al-Gethami, D. Alhashmialameer, N. Al-Qasmi, S. H. Ismail and A. H. Sadek, *Nanomaterials*, 2022, **12**, 3620.
49 Q. Y. Tamboli, S. M. Patange, Y. K. Mohanta, A. D. Patil, R. Ali, I. Bushnak and K. Zakde, *ACS Omega*, 2024, **9**, 3835–3845.
50 D. Gingasu, I. Mindru, D. C. Culita, J. M. Calderon-Moreno, C. Bartha, S. Greculeasa, N. Iacob, S. Preda and O. Oprea, *Appl. Phys. A*, 2021, **127**, 892.
51 B. Basha, M. Ikram, Z. A. Alrowaili, M. S. Al-Buriahi, M. Anwar and M. Suleman, *Ceram. Int.*, 2023, **49**, 30049–30059.
52 K. V. Siva, A. Kumar and A. Arockiarajan, *J. Magn. Magn. Mater.*, 2021, **535**, 168065.
53 R. I. Shakirzyanov, A. L. Kozlovskiy, M. V. Zdorovets, A. L. Zheludkevich, D. I. Shlimas, N. V. Abmiotka, P. A. Kazantsev, T. I. Zubar, S. V. Trukhanov and A. V. Trukhanov, *J. Alloys Compd.*, 2023, **954**, 170083.
54 G. He, J. Ding, J. Zhang, Q. Hao and H. Chen, *Ind. Eng. Chem. Res.*, 2015, **54**, 2862–2867.
55 A. M. El Shafey, *Green Process. Synth.*, 2020, **9**, 304–339.
56 V. Soni, P. Raizada, P. Singh, H. N. Cuong, R. S, A. Saini, R. V Saini, Q. Van Le, A. K. Nadda, T.-T. Le and V.-H. Nguyen, *Environ. Res.*, 2021, **202**, 111622.
57 M. I. Din, F. Rafique, M. S. Hussain, H. A. Mehmood and S. Waseem, *Sci. Prog.*, 2019, **102**, 61–72.
58 T. Van Tran, D. T. C. Nguyen, P. S. Kumar, A. T. M. Din, A. A. Jalil and D.-V. N. Vo, *Environ. Chem. Lett.*, 2022, **20**, 1309–1331.
59 H. ter Steege, N. C. A. Pitman, D. Sabatier and E. Al, *Science*, 2013, **342**, 1243092.
60 W. Wang, J. Wang, F. M. P. Choi, P. Ding, X. Li, G. Han, M. Ding, M. Guo, X. Huang, W. Duan, Z. Cheng, Z. Chen, S. J. Hawkins, Y. Jiang, B. Helmuth and Y. Dong, *Glob. Ecol. Biogeogr.*, 2020, **29**, 220–231.
61 M. Pirsaheb, T. Gholami, H. Seifi, E. A. Dawi, E. A. Said, A.-H. M. Hamoody, U. S. Altimari and M. Salavati-Niasari, *Environ. Sci. Pollut. Res.*, 2024, **31**, 24768–24787.
62 D. Gingasu, I. Mindru, L. Patron, J. M. Calderon-Moreno, O. C. Mocioiu, S. Preda, N. Stanica, S. Nita, N. Dobre, M. Popa, G. Gradisteanu and M. C. Chifiriuc, *J. Nanomater.*, 2016, **2016**, 1–12.
63 K. Kombaiah, J. J. Vijaya, L. J. Kennedy, M. Bououdina, R. J. Ramalingam and H. A. Al-Lohedan, *Ceram. Int.*, 2017, **43**, 7682–7689.
64 A. Manikandan, R. Sridhar, S. A. Antony and S. Ramakrishna, *J. Mol. Struct.*, 2014, **1076**, 188–200.
65 G. C. Hermosa, C.-S. Liao, H.-S. Wu, S.-F. Wang, T.-Y. Liu, K.-S. Jeng, S.-S. Lin, C.-F. Chang and A.-C. A. Sun, *IEEE Trans. Magn.*, 2022, **58**, 1–7.
66 K. L. Routray, S. Saha and D. Behera, *Mater. Chem. Phys.*, 2019, **224**, 29–35.
67 M. Duque-Acevedo, L. J. Belmonte-Urena, F. J. Cortés-García and F. Camacho-Ferre, *Glob. Ecol. Conserv.*, 2020, **22**, e00902.
68 B. Koul, M. Yakoob and M. P. Shah, *Environ. Res.*, 2022, **206**, 112285.
69 Rahmayeni, A. Alfina, Y. Stiadi, H. J. Lee and Zulhadjri, *Mater. Res.*, 2019, **22**, 0228.
70 T. Tatarchuk, N. Danyliuk, A. Shyichuk, V. Kotsyubynsky, I. Lapchuk and V. Mandzyuk, *Emergent Mater.*, 2022, **5**, 89–103.
71 N. T. T. Nguyen, L. M. Nguyen, T. T. T. Nguyen, T. T. Nguyen, D. T. C. Nguyen and T. Van Tran, *Environ. Chem. Lett.*, 2022, **20**, 2531–2571.
72 M. Ovais, A. T. Khalil, N. U. Islam, I. Ahmad, M. Ayaz, M. Saravanan, Z. K. Shinwari and S. Mukherjee, *Appl. Microbiol. Biotechnol.*, 2018, **102**, 6799–6814.
73 P. Kushwaha and P. Chauhan, *Inorg. Nano-Met. Chem.*, 2021, 1–8.
74 N. Bao, L. Shen, W. An, P. Padhan, C. H. Turner and A. Gupta, *Chem. Mater.*, 2009, **21**, 3458–3468.

75 M. Adibi, S. M. Mirkazemi and S. Alamolhoda, *Appl. Phys. A*, 2021, **127**, 497.
76 I. A. Fernandes de Medeiros, A. L. Lopes-Moriyama and C. P. de Souza, *Ceram. Int.*, 2017, **43**, 3962–3969.
77 O. Baytar, A. Ekinci, Ö. Şahin and A. Akdag, *ChemistrySelect*, 2024, **9**, e202304491.
78 K. Kombaiah, J. J. Vijaya, L. J. Kennedy, M. Bououdina and B. Al Najar, *J. Alloys Compd.*, 2018, **735**, 1536–1545.
79 F. V. de Andrade, A. B. de Oliveira, G. O. Siqueira, M. M. Lage, M. R. de Freitas, G. M. de Lima and J. Nuncira, *J. Environ. Chem. Eng.*, 2021, **9**, 106232.
80 R. E. Nimshi, J. J. Vijaya, L. J. Kennedy, P. S. Selvamani, M. Bououdina and P. J. Sophia, *Ceram. Int.*, 2023, **49**, 13762–13773.
81 R. Kavitha, K. K. Veni, S. Sagadevan and L. C. Nehru, *Ceram. Int.*, 2024, **50**, 4861–4874.
82 A. Miri, M. Sarani, A. Najafidoust, M. Mehrabani, F. A. Zadeh and R. S. Varma, *Mater. Res. Bull.*, 2022, **149**, 111706.
83 Nitika, A. Rana, V. Kumar and A. M. Awasthi, *Ceram. Int.*, 2021, **47**, 20669–20677.
84 K. Sudarmozhi, D. Iranian and N. Alessa, *Alexandria Eng. J.*, 2024, **94**, 366–376.
85 H. D. T. Duong, D. T. Nguyen and K.-S. Kim, *Nanomaterials*, 2021, **11**, 3056.
86 F. R. Mariosi, J. Venturini, A. da Cas Viegas and C. P. Bergmann, *Ceram. Int.*, 2020, **46**, 2772–2779.
87 S. Zhai, J. Liu, J. Sheng, J. Xu and H. Jiang, *Chem. Eng. J.*, 2021, **421**, 130403.
88 M. Chakraborty, R. Thangavel, A. Biswas and G. Udayabhanu, *CrystEngComm*, 2016, **18**, 3095–3103.
89 K. Habanjar, H. Shehabi, A. M. Abdallah and R. Awad, *Appl. Phys. A*, 2020, **126**, 402.
90 P. Thakur, D. Chahar, S. Taneja, N. Bhalla and A. Thakur, *Ceram. Int.*, 2020, **46**, 15740–15763.
91 A. Franco, F. C. e Silva and V. S. Zapf, *J. Appl. Phys.*, 2012, **111**, 07B530.
92 R. Verma, A. Chauhan, Neha, K. M. Batoo, R. Kumar, M. Hadhi and E. H. Raslan, *Ceram. Int.*, 2021, **47**, 3680–3691.
93 X. Li, Y. Sun, Y. Zong, Y. Wei, X. Liu, X. Li, Y. Peng and X. Zheng, *J. Alloys Compd.*, 2020, **841**, 155710.
94 R. Lamouri, O. Mounkachi, E. Salmani, M. Hamedoun, A. Benyoussef and H. Ez-Zahraouy, *Ceram. Int.*, 2020, **46**, 8092–8096.
95 H. M. Do, T. H. P. Le, D. T. Tran, T. N. A. Nguyen, I. Skorvanek, J. Kovac, P. Svec and M. H. Phan, *J. Sci.: Adv. Mater. Devices*, 2024, **9**, 100658.
96 S. S. Banifatemi, F. Davar, B. Aghabarari, J. A. Segura, F. J. Alonso and S. M. Ghoreishi, *Ceram. Int.*, 2021, **47**, 19198–19204.
97 P. Fan, W. Tan and H. Yu, *Ecotoxicol. Environ. Saf.*, 2022, **229**, 113045.
98 M. De Palma, R. Scotti, N. D'Agostino, M. Zaccardelli and M. Tucci, *Plants*, 2022, **11**, 2672.
99 A. Sehrawat, S. S. Sindhu and B. R. Glick, *Pedosphere*, 2022, **32**, 15–38.
100 M. S. Lionakis, R. A. Drummond and T. M. Hohl, *Nat. Rev. Immunol.*, 2023, **23**, 433–452.
101 T.-Z. Jing, F.-H. Qi and Z.-Y. Wang, *Microbiome*, 2020, **8**, 38.
102 S. Mukherjee, S. Barman, R. Mukherjee and J. Haldar, *Front. Bioeng. Biotechnol.*, 2020, **8**, 00055.
103 K. Ni, G. Lan and W. Lin, *ACS Cent. Sci.*, 2020, **6**, 861–868.
104 G. Palanisamy, K. Bhuvaneswari, A. Chinnadurai, G. Bharathi and T. Pazhanivel, *J. Phys. Chem. Solids*, 2020, **138**, 109231.
105 S. Kalia, V. Dhiman, T. T. T. Carol, D. Basandrai and N. Prasad, *Inorg. Chem. Commun.*, 2023, **150**, 110382.
106 K. Khalid, A. Zahra, U. Amara, M. Khalid, M. Hanif, M. Aziz, K. Mahmood, M. Ajmal, M. Asif, K. Saeed, M. F. Qayyum and W. Abbas, *Chemosphere*, 2023, **338**, 139531.
107 E. Fantechi, C. Innocenti, M. Zanardelli, M. Fittipaldi, E. Falvo, M. Carbo, V. Shullani, L. Di Cesare Mannelli, C. Ghelardini, A. M. Ferretti, A. Ponti, C. Sangregorio and P. Ceci, *ACS Nano*, 2014, **8**, 4705–4719.
108 S. Hatamie, Z. M. Balasi, M. M. Ahadian, T. Mortezazadeh, F. Shams and S. Hosseinzadeh, *J. Drug Deliv. Sci. Technol.*, 2021, **65**, 102680.
109 P. B. Balakrishnan, N. Silvestri, T. Fernandez-Cabada, F. Marinaro, S. Fernandes, S. Fiorito, M. Miscuglio, D. Serantes, S. Ruta, K. Livesey, O. Hovorka, R. Chantrell and T. Pellegrino, *Adv. Mater.*, 2020, **32**, 2003712.
110 Y. Wang, L. Zou, Z. Qiang, J. Jiang, Z. Zhu and J. Ren, *ACS Biomater. Sci. Eng.*, 2020, **6**, 3550–3562.
111 G. Nandhini and M. K. Shobana, *J. Magn. Magn. Mater.*, 2022, **552**, 169236.
112 D. L. Puspitarum, N. I. Istiqomah, R. M. Tumbelaka, A. Kusumaatmaja, D. Oshima, T. Kato and E. Suharyadi, *Adv. Nat. Sci.: Nanosci. Nanotechnol.*, 2022, **13**, 045003.
113 H. Yang, *Mater. Res. Bull.*, 2021, **142**, 111406.
114 M. Liaskovska, T. Tatarchuk, V. Kotsyubynsky and H. Ersteniuk, *Phys. Chem. Solid State*, 2021, **22**, 792–803.
115 S. J. Olusegun and N. D. S. Mohallem, *Environ. Pollut.*, 2020, **260**, 114019.
116 H. Cao, R. Wang, K. Dou, J. Qiu, C. Peng, N. Tsidaeva and W. Wang, *Environ. Res.*, 2023, **216**, 114730.
117 H. Tasqeen, M. Waseem, S. Hussain, Zil-E-Humma, A. Baig and A. Majeed, *Chem. Pap.*, 2024, **78**, 4517–4528.
118 J. R. P. Oliveira, L. S. Ribas, J. S. Napoli, E. Abreu, J. L. Diaz de Tuesta, H. T. Gomes, A. M. Tusset and G. G. Lenzi, *Magnetochemistry*, 2023, **9**, 200.
119 W. A. Al-Amrani and S. A. Onaizi, *Sep. Purif. Technol.*, 2024, **343**, 127018.
120 P. Apostoli, S. Catalani, A. Zaghini, A. Mariotti, P. L. Poliani, V. Vielmi, F. Semeraro, S. Duse, A. Porzionato, V. Macchi, A. Padovani, M. C. Rizzetti and R. De Caro, *Exp. Toxicol. Pathol.*, 2013, **65**, 719–727.